Free vibration analysis of multi-cracked micro beams based on Modified Couple Stress Theory

Abbas Rahi [*a], **Hamed Petoft** [b]

[a] *Assistant Professor, Mechanical & Energy Engineering, Shahid Beheshti University, A.C., Tehran, Iran*

[b] *Ph.D. Candidate, Faculty of Mechanical & Energy Engineering, Shahid Beheshti University, A.C., Tehran, Iran*

ARTICLE INFO

ABSTRACT

In this article, the size effect on the dynamic behavior of a simply supported multi-cracked microbeam is studied based on Modified Couple Stress Theory (MCST). At first, based on MCST, the equivalent torsional stiffness spring for every open edge crack at its location is calculated; in this regard, the Stress Intensity Factor (SIF) is also considered for all open edge cracks. Hamilton's principle has been used in order to achieve the governing equations of motion of the system and associated boundary conditions are derived based on MCST. Then the natural frequencies of multi-cracked microbeam are analytically determined. After that, the Numerical solutions have been presented for the microbeam with two open edge cracks. Finally, the variation of the first three natural frequencies of the system is investigated versus different values of the depth and the location of two cracks and the material length scale parameter. The obtained results express that the natural frequencies of the system increase by increasing the material length scale parameter and decrease by moving away from the simply supported of the beam and node points, in addition to increasing the number of cracks and cracks depth.

1. Introduction

Nowadays, because of the development of new technologies, approaches to design and research about small size structures have been increased more than ever. Micro and nanostructures such as microbeams are one of the most common important components, which are used in the micro-

---

electromechanical systems (MEMS) such as microswitches. [1, 2]There are several studies on microbeams using the size-dependent theories. Kong *et al*.[3] showed the size effect of microbeam in the natural frequency of the system. They used Euler-Bernoulli model for the beam and analytically solved the dynamical problem of the system using Modified Couple Stress Theory (MCST). Park and Gao[4] also used MCST with Euler-Bernoulli model for bending of a cantilever beam. Dado and Abuzeid [5] investigated about coupled transverse and axial vibratory behavior of cracked beam with a concentrated mass and rotary inertia at end of the beam. Al-Basyouni *et al*. [6]studied vibration analysis of Functionally Graded (FG) microbeams based on MCST. Li *et al*.[7] investigated on bending, buckling and vibration analysis of axially FG a Euler-Bernoulli microbeam based on the nonlocal strain gradient theory. In other words, the scale parameter changes during the length of the beam. They derived the equations of motion from Hamilton's principle and for solving the equations used a Generalized Differential Quadrature Method (GDQM). The influences of power-law variation and size-dependent parameters have also been investigated on the bending, buckling and vibration behaviors of axially FG beams. Shafiei *et al*. [8]obtained equations for transverse vibration of rotary tapered microbeam. Zhang and Wang[9] showed exact controllability and observability of a microbeam with the boundary-bending moment. Fang *et al*. [10]presented governing equations of three-dimensional free vibration of rotating FG microbeams based on MCST using Euler-Bernoulli beam theory. Babaei *et al*.[11] also investigated on free vibration analysis of an FG microbeam based on MCST using Euler-Bernoulli model and considering thermal effect. Recently, Taati and Sina [12] utilized Multi-objective optimization of distribution parameter of FGM, thickness and aspect ratio in a microbeam embedded in an elastic medium in order to minimize and maximum deflection, maximum stress and mass and maximizing values of natural frequency and critical buckling load.

On the other hand, the problem of the damage of structures cannot be ignored. One of the most important faults in a structure is the existence of cracks, especially in small structures. Often, in research, crack is modeled with a torsional spring and the effect of crack existence is investigated on the natural frequency of vibrational systems and component's life. Some research has examined the impact of just one crack in the system. Akbarzadeh and Shariati [13] presented analytical solutions of a critical buckling load and the post-buckling response for an open edge cracked microbeam with simply-supported boundary conditions based on MCST with Euler-Bernoulli's model. They also studied a cracked Timoshenko Nano-beam and considered coupled effects between the axial force and bending moment by two equivalent springs.[14] Alsabbagh *et al*. [15]introduced simplified formula for the stress correction factor in terms of the crack depth to the beam height ratio. Panigrahi and Pohit [16] researched about the effect of a crack on the nonlinear vibration of rotating FGM cantilever beam having large motion based on the Timoshenko's beam model. Soltanpour *et al*. [17] investigated equations of free transverse vibration of an FG cracked nano-beam resting on elastic medium with Timoshenko's model with simply supported-simply supported (SS) and Clamped-Clamped (CC) boundary conditions. Akbas[18] presented analytical and numerical solutions for free vibration of a cracked FG cantilever microbeam based on MCST with Euler-Bernoulli's model. Huyen and Khiem[19] investigated frequency analysis of a cracked FG cantilever beam. Behera *et al*.[20] investigated the influence of crack incline on first three mode shapes of a cantilever beam. Moreover, they verified numerical solutions with experimental test results. Rahi [21] investigated the lateral vibration of a cracked simply-supported microbeam based on MCST. He presented four models

for Stress Intensity Factor (SIF) and compared them in his numerical results and showed the effect of the crack depth ratio η, the crack location L_C and material length scale parameter l on the equivalent torsional stiffness of the crack and first two natural frequencies of the system. Nakhaei *et al*. [22] presented some models for a beam with a breathing crack with two different circulars and V-shape for the shape of the crack. Then, effects of the crack's parameters which include depth, shape, and location on the first natural frequency of the system were investigated. Fu *et al*. [23] studied on a simply-supported cracked beam considering nonlinear stress distributions near the crack with two different T-shape and rectangular cross-sections for the beam and then, presented an estimation for local and global stiffness. In addition, another interesting approach for researchers is crack detection (for one crack or multiple cracks) and recently, there are many studies on this subject.[24-33]

Another group of studies is about beams with multiple cracks. Shoaib *et al*. [34] investigated on effects of single and double edge crack on the dynamics of piezoelectric cantilever-based MEMS sensor. Khiem and Hung[35] used a closed-form solution for free vibration of multiple cracked Timoshenko beam with various boundary conditions. Cannizzaro *et al*. [36] presented closed-form solutions for multi-cracked circular arch beam under concentrated static loads. Yoon *et al*. [37]investigated the influence of two open cracks on the dynamic behavior of a double cracked simply supported beam both analytically and experimentally. Lien *et al*. [38] presented first three mode shapes of a multiple cracked FG Timoshenko beam for different boundary conditions.

According to mentioned researches, the effect of multiple cracks fault in microbeams has not been investigated until now. In this article, a simply-supported microbeam with multiple open edge cracks is considered. then the governing equations with the corresponding boundary conditions are obtained based on MCST using an analytical approach. and present Afterward, in the case study, a cracked microbeam with two cracks is studied. Finally, the effect of the position and depth of the cracks and also material-length-scale parameter on the first three natural frequencies of the system are investigated.

Therefore, the main contribution of the article is investigating the effect of multiple cracks on the free vibration of micro-beams with Simply-Supported (SS) boundary condition. In addition, in this paper, a general solution is presented by using a logical algorithm for determining boundary conditions of the microbeam with multiple cracks. In other words, natural frequencies of the multi-crack micro-beam calculated analytically for the first time.

2. Multi-cracked microbeam modeling

Consider a microbeam with n cracks in which crack number i has depth a_i and location L_{c_i} from the left support. Microbeam has the rectangular cross-section, with width b, height h, length L, with the coordinate system X-Y-Z as shown in Fig. 1. The open edge cracks are assumed perpendicular to the neutral axis of the microbeam and non-propagating.
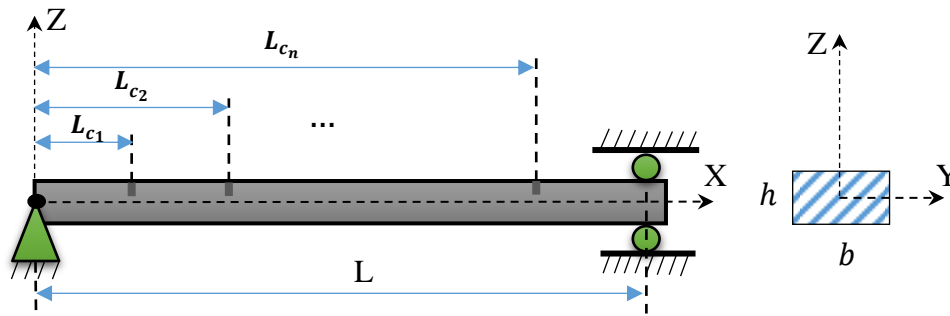
Fig. 1: Microbeam with multiple open edge cracks

According to the number of cracks, lateral displacement of microbeam is divided into $n + 1$ segments and every segment has a specific function of displacement. In other words, displacement of the beam includes $n + 1$ separate functions of the displacement and time.

Every crack can be modeled with torsional spring such that each of them has a torsional stiffness. It can be said in another way that for analysis of the lateral vibration, the multi-crack microbeam can be modeled in $n + 1$ segments which are connected to them with torsional springs at locations $L_{c_1}, L_{c_2} \ldots L_{c_n}$ (please see Fig. 2). According to Fig. 2, cracks are modeled with torsional springs with equivalent torsional stiffness $K_{t_1}, K_{t_2}, \ldots, K_{t_n}$.
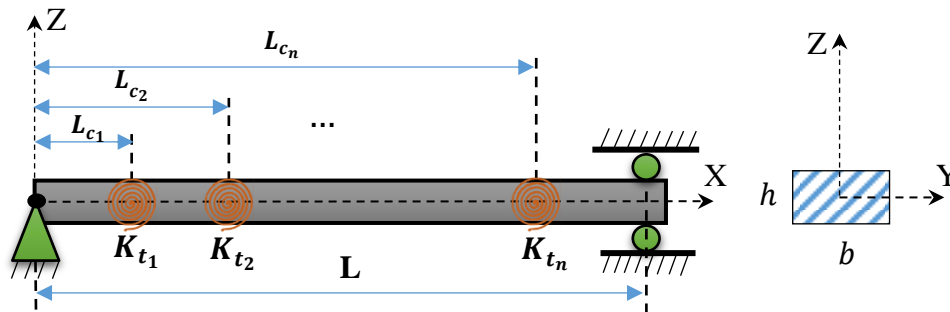

Fig. 2: Modeling of open edge cracks with torsional springs

3. Calculation of the equivalent torsional stiffness of cracks

According to the reference [21], which has presented new models for calculating local stiffness with considering the Stress Intensity Factor (SIF), the equivalent torsional stiffness for every crack can be written as follows:

$$K_t = \frac{1}{C} = \frac{1}{\left[1 + \frac{6}{(1+\vartheta)(1-\eta)^2}\left(\frac{l}{h}\right)^2\right]} \left[\frac{EI}{6\pi h(1-\vartheta^2)D}\right] \tag{1}$$

where

$$D = 19.600\eta^{10} - 40.693\eta^9 + 47.041\eta^8 - 33.153\eta^7 + 20.469\eta^6 - 10.092\eta^5 + 4.631\eta^4 \\ - 1.077\eta^3 + 0.629\eta^2 \tag{2}$$

where η is non-dimensional coefficient which is defined as the ratio of crack depth a to the height of cross-section of the microbeam h or $\eta = \frac{a}{h}$.

4. Governing equations of motion

According to the previous sections, by assuming the material properties Young's modulus E, Poisson's ratio ϑ, density ρ, cross-section area moment of inertia I and material length scale parameter l, the strain energy π_s of each segment of the microbeam can be written as follows [21]:

$$\pi_s = \frac{1}{2}EI\int_0^L \left(\frac{\partial^2 w}{\partial x^2}\right)^2 dx + \frac{1}{2}\frac{6EI}{1+\vartheta}\left(\frac{l}{h}\right)^2 \int_0^L \left(\frac{\partial^2 w}{\partial x^2}\right)^2 dx \tag{3}$$

where A denotes cross-section of the microbeam, and $I = \int_A z^2\, dA = \frac{bh^3}{12} = \frac{Ah^2}{12}$ denotes the cross section area-moment of inertia.

The kinetic energy of the system T can also be written as follows:

$$T = \frac{\rho}{2}\int_0^L [A\dot{w}^2]\, dx \tag{4}$$

where ρ is the density of the microbeam.

Based on Hamilton's principle, which is as follows:

$$\int_{t_1}^{t_2} \delta(T - \pi + W)\, dt = 0 \tag{5}$$

By substituting the Eqs. (3) and (4) into (5), and after simplifying by using variation calculus, governing equations of each segment of the microbeam can be derived as follows:

$$S\frac{\partial^4 w}{\partial x^4} + \rho A\ddot{w} = 0 \tag{6}$$

where

$$S = EI\left[1 + \frac{6}{1+\vartheta}\left(\frac{l}{h}\right)^2\right] \tag{7}$$

The solution of Eq. (6) can be written as follows:

$$w(x, t) = W(x) . sin(\omega t)$$

(8)

By substituting Eq. (8) into Eq. (6) and with some algebraic simplification, we have

$$\frac{d^4 W}{dx^4} - \beta^4 W(x) = 0$$

(9)

$$\beta^4 = \frac{\rho A \omega^2}{S}$$

where ω is natural frequency, ρ is the material density of the microbeam, and A is the cross-section of the microbeam.

Also, the general solution of Eq. (9) for each segment can be obtained as follows:

$$W(x) = A_1 \sin(\beta x) + A_2 \cos(\beta x) + A_3 \sinh(\beta x) + A_4 \cosh(\beta x)$$

(10)

where A_i , $(i = 1, 2, 3, 4)$ are constants.

Equation (10) can be utilized for every segment and therefore, the governing equations of motion of the first to final n+1 segment, respectively, can be written as follows

$$W_1(x) = \tilde{A}_1 \sin(\beta x) + \tilde{A}_2 \cos(\beta x) + \tilde{A}_3 \sinh(\beta x) + \tilde{A}_4 \cosh(\beta x) ; \ 0 \le x \le L_{c1}$$

$$W_2(x) = \tilde{A}_5 \sin(\beta x) + \tilde{A}_6 \cos(\beta x) + \tilde{A}_7 \sinh(\beta x) + \tilde{A}_8 \cosh(\beta x) ; \ L_{c1} \le x \le L_{c2}$$

$$\vdots \qquad \qquad \vdots \qquad \qquad \vdots$$

(11)

$$W_{n+1}(x) = \tilde{A}_{4n+1} \sin(\beta x) + \tilde{A}_{4n+2} \cos(\beta x) + \tilde{A}_{4n+3} \sinh(\beta x)$$
$$+ \tilde{A}_{4(n+1)} \cosh(\beta x) \ ; \qquad \qquad L_{cn} \le x \le L$$

where $\tilde{A}_1$ to $\tilde{A}_{4(n+1)}$ are constants and L_{cn} is location of the crack number n. By assuming L_{ci} as the crack location of i $(i = 1, 2, \dots , n)$, the boundary conditions of the system can be expressed as follows:

$$W_1(0) = 0 \ ; \ \frac{d^2 w_1}{dx^2}(0) = 0$$

(12)

$$W_{n+1}(L) = 0 \ ; \ \frac{d^2 w_{n+1}}{dx^2}(L) = 0$$

$$W_i(L_{ci}) = W_{i+1}(L_{ci})$$

$$\frac{dw_{i+1}}{dx}(L_{ci})) - \frac{dw_i}{dx}(L_{ci}) = \frac{d^2 w_i}{dx^2}(L_{ci}) \times \frac{S}{K_{ti}}$$

$$S \frac{d^2 w_i}{dx^2}(L_{ci}) = S \frac{d^2 w_{i+1}}{dx^2}(L_{ci})$$

(13)

$$S \frac{d^3 w_i}{dx^3}(L_{ci}) = S \frac{d^3 w_{i+1}}{dx^3}(L_{ci})$$

where K_{ti} is the equivalent torsional stiffness spring of the microbeam at i-th crack's location.

By substituting Eqs. (13) and (12) into Eq. (11), a set of $4(n + 1)$ algebraic equations resulting in matrix form for n cracks can be written as follows:

$$[Q(i,j)]\{\tilde{A}_j\} = 0 \quad ; \quad i, j = 1, \quad 2, \dots, 4(n+1) \tag{14}$$

where the non-zero components of matrix $[Q]$ can be expressed as follows:

$$Q(1,2) = 1 \; ; \quad Q(1,4) = 1$$

$$Q(2,2) = -\beta^2; \quad Q(2,4) = \beta^2$$

$$Q(3,4n+1) = \sin(\beta L) \; ; \quad Q(3,4n+2) = \cos(\beta L)$$

$$Q(3,4n+3) = \sinh(\beta L) \; ; \quad Q(3,4(n+1)) = \cosh(\beta L)$$

$$Q(4,4n+1) = -\beta^2 \sin(\beta L) \; ; \quad Q(4,4n+2) = -\beta^2 \cos(\beta L)$$

$$Q(4,4n+3) = \beta^2 \sinh(\beta L) \; ; \quad Q(4,4(n+1)) = \beta^2 \cosh(\beta L)$$

$$Q(4+k,4k-3) = \sin(\beta L_{ck}) \; ; \quad Q(4+k,4k-2) = \cos(\beta L_{ck})$$

$$Q(4+k,4k-1) = \sinh(\beta L_{ck}) \; ; \quad Q(4+k,4k) = \cosh(\beta L_{ck})$$

$$Q(4+k,4k+1) = -\sin(\beta L_{ck}) \; ; \quad Q(4+k,4k+2) = -\cos(\beta L_{ck})$$

$$Q(4+k,4k+3) = -\sinh(\beta L_{ck}) \; ; \quad Q(4+k,4(k+1)) = -\cosh(\beta L_{ck})$$

$$Q(4+n+k,4k-3) = \beta \cos(\beta L_{ck}) - \frac{S\beta^2}{K_{tk}} \sin(\beta L_{ck})$$

$$Q(4+n+k,4k-2) = -\beta \sin(\beta L_{ck}) - \frac{S\beta^2}{K_{tk}} \cos(\beta L_{ck})$$

$$Q(4+n+k,4k-1) = \beta \cosh(\beta L_{ck}) + \frac{S\beta^2}{K_{tk}} \sinh(\beta L_{ck}) \tag{15}$$

$$Q(4+n+k,4k) = \beta \sinh(\beta L_{ck}) + \frac{S\beta^2}{K_{tk}} \cosh(\beta L_{ck})$$

$$Q(4+n+k,4k+1) = -\beta \cos(\beta L_{ck}) \; ; \quad Q(4+n+k,4k+2) = \beta \sin(\beta L_{ck})$$

$$Q(4+n+k,4k+3) = -\beta \cosh(\beta L_{ck}) \; ; \quad Q(4+n+k,4(k+1)) = -\beta \sinh(\beta L_{ck})$$

$$Q(4+2n+k,4k-3) = -\beta^2 \sin(\beta L_{ck}) \; ; \quad Q(4+2n+k,4k-2) = -\beta^2 \cos(\beta L_{ck})$$

$$Q(4+2n+k,4k-1) = \beta^2 \sinh(\beta L_{ck}) \; ; \quad Q(4+2n+k,4k) = \beta^2 \cosh(\beta L_{ck})$$

$$Q(4+2n+k,4k+1) = \beta^2 \sin(\beta L_{ck}) \; ; \quad Q(4+2n+k,4k+2) = \beta^2 \cos(\beta L_{ck})$$

$$(4+2n+k,4k+3) = -\beta^2 \sinh(\beta L_{ck}) \; ; \quad Q(4+2n+k,4(k+1)) = -\beta^2 \cosh(\beta L_{ck})$$

$$Q(4+3n+k,4k-3) = -\beta^3 \cos(\beta L_{ck}) \; ; \quad Q(4+3n+k,4k-2) = \beta^3 \sin(\beta L_{ck})$$

$$Q(4+3n+k,4k-1) = \beta^3 \cosh(\beta L_{ck}) \; ; \quad Q(4+3n+k,4k) = \beta^3 \sinh(\beta L_{ck})$$

$$Q(4+3n+k,4k+1) = \beta^3 \cos(\beta L_{ck}) \; ; \quad Q(4+3n+k,4k+2) = -\beta^3 \sin(\beta L_{ck})$$

$$Q(4+3n+k,4k+3) = -\beta^3 \cosh(\beta L_{ck}) \; ; \quad Q(4+3n+k,4(k+1)) = -\beta^3 \sinh(\beta L_{ck})$$

where $k = 1, 2, \ldots n$.

For the nontrivial solution of Eq. (14), the determinant of the matrix $[Q]$ must be zero. The obtained results are natural frequencies of the system, which can be calculated by semi-analytical or numerical methods.

5. Case study: A microbeam with two cracks

According to Eqs. (12), (13), by assuming two cracks in the microbeam, the boundary conditions of the system can be rewritten as follows:

$$W_1(0) = 0 \;\; ; \;\; \frac{d^2 w_1}{dx^2}(0) = 0$$

$$W_3(L) = 0 \;\; ; \;\; \frac{d^2 w_3}{dx^2}(L) = 0$$

$$W_1(L_{c1}) = W_2(L_{c1}) \;\; ; \;\; W_2(L_{c2}) = W_3(L_{c2})$$

$$\frac{dw_2}{dx}(L_{c1}) - \frac{dw_1}{dx}(L_{c1}) = \frac{d^2 w_1}{dx^2}(L_{c1}) \times \frac{S}{K_{t1}}$$

$$\frac{dw_3}{dx}(L_{c2}) - \frac{dw_2}{dx}(L_{c2}) = \frac{d^2 w_2}{dx^2}(L_{c2}) \times \frac{S}{K_{t2}}$$

$$S\frac{d^2 w_1}{dx^2}(L_{c1}) = S\frac{d^2 w_2}{dx^2}(L_{c1}) \;\; ; \;\; S\frac{d^2 w_2}{dx^2}(L_{c2}) = S\frac{d^2 w_3}{dx^2}(L_{c2})$$

$$S\frac{d^3 w_1}{dx^3}(L_{c1}) = S\frac{d^3 w_2}{dx^3}(L_{c1}) \;\; ; \;\; S\frac{d^3 w_2}{dx^3}(L_{c2}) = S\frac{d^3 w_3}{dx^3}(L_{c2})$$

(16)

According to Eq. (16), for two cracks we have 12 boundary conditions, this means that matrix Q has 12 rows and 12 columns or $[Q]_{12 \times 12}$. Therefore, non-zero components of matrix Q can be simple as follows:

$$Q(1,2) = 1 \;\;\; ; \;\; Q(1,4) = 1$$

$$Q(2,2) = -\beta^2 ; \;\; Q(2,4) = \beta^2$$

$$Q(3,9) = sin(\beta L) ; \;\; Q(3,10) = cos(\beta L)$$

$$Q(3,11) = sinh(\beta L) ; \;\; Q(3,12) = cosh(\beta L)$$

$$Q(4,9) = -\beta^2 sin(\beta L) ; \;\; Q(4,10) = -\beta^2 cos(\beta L)$$

$$Q(4,11) = \beta^2 sinh(\beta L) ; \;\; Q(4,12) = \beta^2 cosh(\beta L) Q(5,1) = sin(\beta L_{c1}) ; \;\; Q(6,5) = sin(\beta L_{c2}) ;$$

$$Q(5,2) = cos(\beta L_{c1}) ; \;\; Q(6,6) = cos(\beta L_{c2})$$

$$Q(5,3) = sinh(\beta L_{c1}) ; \;\; Q(6,7) = sinh(\beta L_{c2}) ;$$

$$Q(5,4) = cosh(\beta L_{c1}) ; \;\; Q(6,8) = cosh(\beta L_{c2})$$

$$Q(5,5) = -sin(\beta L_{c1}) ; \;\; Q(6,9) = -sin(\beta L_{c2}) ;$$

$$Q(5,6) = -cos(\beta L_{c1}) ; \;\; Q(6,10) = -cos(\beta L_{c2})$$

$$Q(5,7) = -sinh(\beta L_{c1}) ; Q(6,11) = -sinh(\beta L_{c2}) ;$$

$$Q(5,8) = -cosh(\beta L_{c1}) ; \;\; Q(6,12) = -cosh(\beta L_{c2})$$

(17)

$$Q(7,1) = \beta \cos(\beta L_{c1}) - \frac{S\beta^2}{K_{t1}} \sin(\beta L_{c1}) \,;$$

$$Q(8,5) = \beta \cos(\beta L_{c2}) - \frac{S\beta^2}{K_{t2}} \sin(\beta L_{c2})$$

$$Q(7,2) = -\beta \sin(\beta L_{c1}) - \frac{S\beta^2}{K_{t1}} \cos(\beta L_{c1}) \,;$$

$$Q(8,6) = -\beta \sin(\beta L_{c2}) - \frac{S\beta^2}{K_{t2}} \cos(\beta L_{c2})$$

$$Q(7,3) = \beta \cosh(\beta L_{c1}) + \frac{S\beta^2}{K_{t1}} \sinh(\beta L_{c1}) \,;$$

$$Q(8,7) = \beta \cosh(\beta L_{c2}) + \frac{S\beta^2}{K_{t2}} \sinh(\beta L_{c2}) \quad Q(7,4) = \beta \sinh(\beta L_{c1}) + \frac{S\beta^2}{K_{t1}} \cosh(\beta L_{c1}) \,;$$

$$Q(8,8) = \beta \sinh(\beta L_{c2}) + \frac{S\beta^2}{K_{t1}} \cosh(\beta L_{c2})$$

$$Q(7,5) = -\beta \cos(\beta L_{c1}) \,; Q(8,9) = -\beta \cos(\beta L_{c1})$$

$$Q(7,6) = \beta \sin(\beta L_{c1}) \,; Q(8,10) = \beta \sin(\beta L_{c2})$$

$$Q(7,7) = -\beta \cosh(\beta L_{c1}) \,; Q(8,11) = -\beta \cosh(\beta L_{c2})$$

$$Q(7,8) = -\beta \sinh(\beta L_{c1}) \,; Q(8,12) = -\beta \sinh(\beta L_{c2})$$

$$Q(9,1) = -\beta^2 \sin(\beta L_{c1}) \,; Q(10,5) = -\beta^2 \sin(\beta L_{c2})$$

$$Q(9,2) = -\beta^2 \cos(\beta L_{c1}) \,; Q(10,6) = -\beta^2 \cos(\beta L_{c2})$$

$$Q(9,3) = \beta^2 \sinh(\beta L_{c1}) \,; Q(10,7) = \beta^2 \sinh(\beta L_{c2})$$

$$Q(9,4) = \beta^2 \cosh(\beta L_{c1}) \,; \ Q(10,8) = \beta^2 \cosh(\beta L_{c2})$$

$$Q(9,5) = \beta^2 \sin(\beta L_{c1}) \,; Q(10,9) = \beta^2 \sin(\beta L_{c2})$$

$$Q(9,6) = \beta^2 \cos(\beta L_{c1}) \,; Q(10,10) = \beta^2 \cos(\beta L_{c2})$$

$$Q(9,7) = -\beta^2 \sinh(\beta L_{c1}) \,; Q(10,11) = -\beta^2 \sinh(\beta L_{c2})$$

$$Q(9,8) = -\beta^2 \cosh(\beta L_{c1}); Q(10,12) = -\beta^2 \cosh(\beta L_{c2})$$

$$Q(11,1) = -\beta^3 \cos(\beta L_{c1}) \,; Q(12,5) = -\beta^3 \cos(\beta L_{c2})$$

$$Q(11,2) = \beta^3 \sin(\beta L_{c1}) \,; Q(12,6) = \beta^3 \sin(\beta L_{c2})$$

$$Q(11,3) = \beta^3 \cosh(\beta L_{c1}) \,; Q(12,7) = \beta^3 \cosh(\beta L_{c2})$$

$$Q(11,4) = \beta^3 \sinh(\beta L_{c1}) \,; Q(12,8) = \beta^3 \sinh(\beta L_{c2})$$

$$Q(11,5) = \beta^3 \cos(\beta L_{c1}) \,; \ Q(12,9) = \beta^3 \cos(\beta L_{c2})$$

$$Q(11,6) = -\beta^3 \sin(\beta L_{c1}) \,; Q(12,10) = -\beta^3 \sin(\beta L_{c2})$$

$$Q(11,7) = -\beta^3 \cosh(\beta L_{c1}) \,; Q(12,11) = -\beta^3 \cosh(\beta L_{c2})$$

$$Q(11,8) = -\beta^3 \sinh(\beta L_{c1}) \,; Q(12,12) = -\beta^3 \sinh(\beta L_{c2})$$

6. Numerical results and discussion

In this section, the numerical method is utilized for solving the problem and obtaining first three natural frequencies of the system. The multi-cracked microbeam is assumed to be made of an epoxy material with the following mechanical properties [21]: Young's modulus $E = 1.44\ GPa$, Poison's ratio $\vartheta = 0.38$, density $\rho = 1220\ \text{kg/m}^3$, and material length scale parameter $l = 17.6\ \mu m$. Also, length and cross-section dimensions of the multi-cracked microbeam are length $L = 20h$, height $h = 20\ \mu m$ and width $b = 2h$.

According to Figs. 1 to 3, the first three natural frequencies of the system $(\omega_{n1}, \omega_{n2}, \omega_{n3})$ have been plotted versus cracks depth ratio (η) with three different material length scale parameter's ratios ($\frac{l}{h} = 0,\ 0.25,\ 0.5$); the location of first and second cracks are fixed at $\frac{L_{c1}}{L} = 0.25$, $\frac{L_{c2}}{L} = 0.5$, respectively. The results show that the natural frequencies increase by increasing material length scale parameter and decrease by increasing cracks depth due to the reduction of the equivalent torsional stiffness K_t.
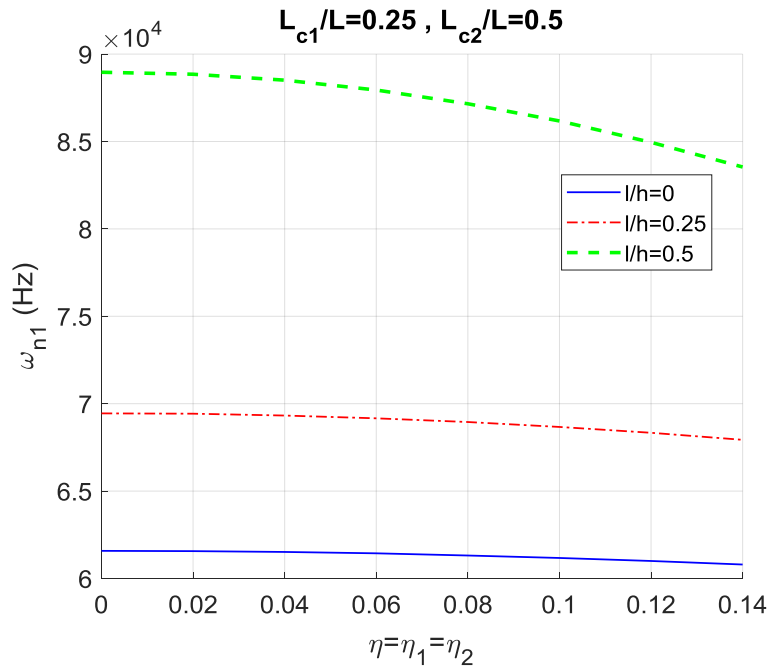

Fig. 3: Variation of the first natural frequency versus the crack depth ratio with three different values of the material-length-scale parameter

Figures 4, 5 and 6, are related to the investigation on the effect of the first crack position and the depth of cracks on the frequencies. The second crack location has been fixed at $\frac{L}{2}$ and material

length scale parameter is constant in the ratio of $\frac{l}{h} = 0.25$. The figures show that the frequencies decrease by increasing the cracks depth and decrease by increasing the number of cracks from the one crack to the two cracks and also generally decrease if the location of the crack moves from the simple supports and node points.
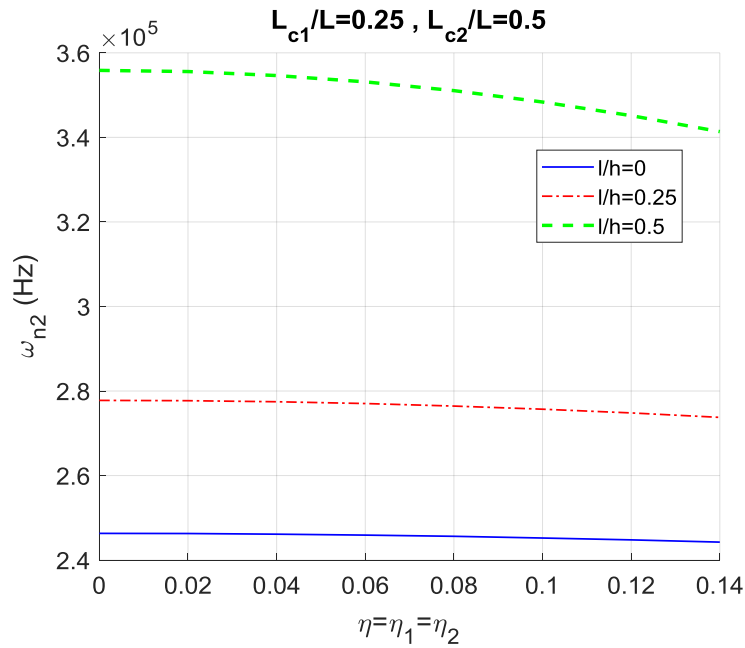

Fig. 4: Variation of the second natural frequency versus the crack depth ratio with three different values of the material-length-scale parameter

In Figs. 9, 10 and 11, the depth of the two cracks is equal and has a constant ratio of $\eta_1 = \eta_2 = 0.2$ and once again, the second crack location has been kept constant at $\frac{L}{2}$ and the first crack location changes from zero to $\frac{L}{2}$ with three different material-length-scale ratios. The obtained results express that the natural frequencies of the system increase by increasing material length scale parameter and decrease by moving away from the simply supported of the beam and node points.
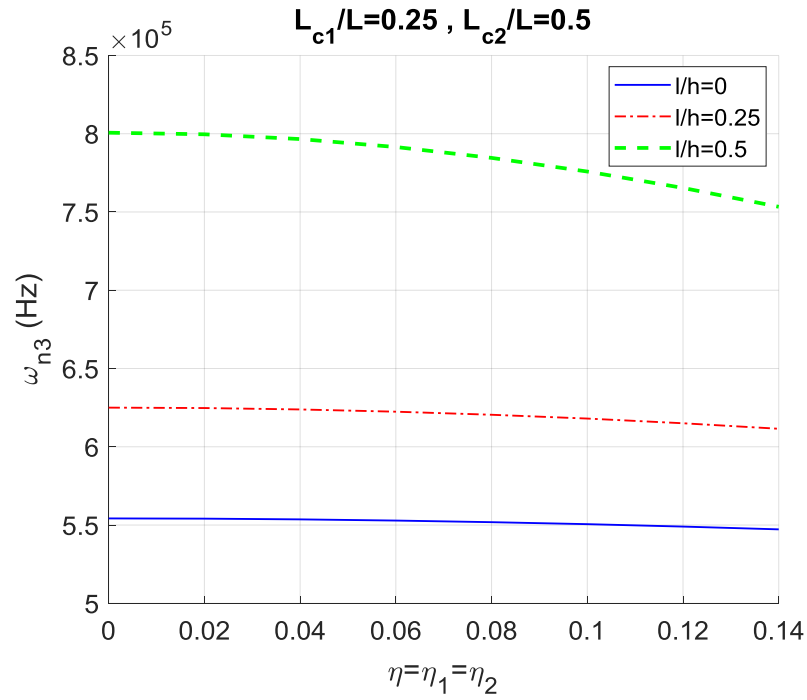
Fig. 5: Variation of the third natural frequency versus the crack depth ratio with three different values of the material-length-scale parameter
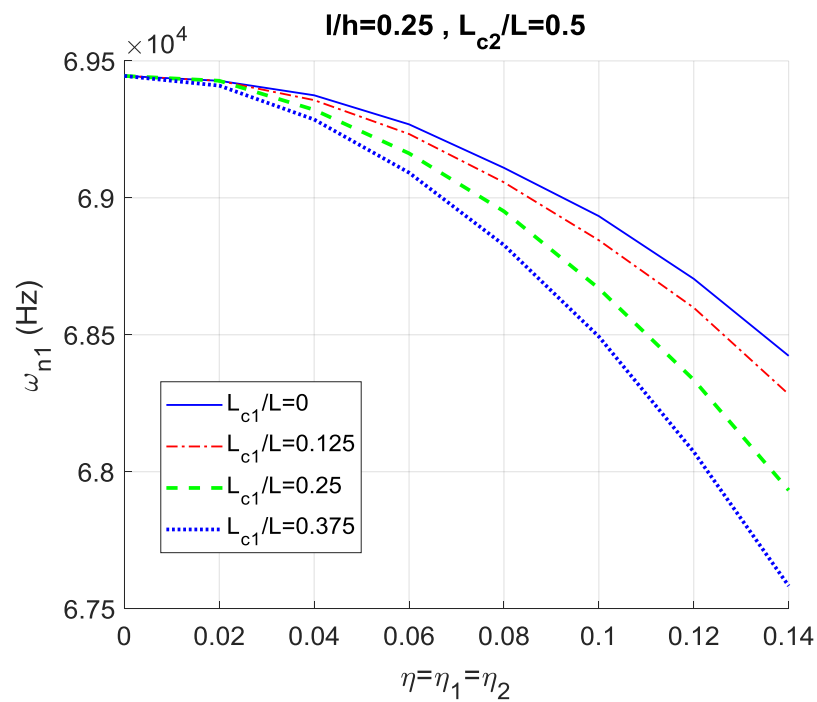

Fig. 6: Variation of the first natural frequency versus the crack depth ratio with the various first crack location
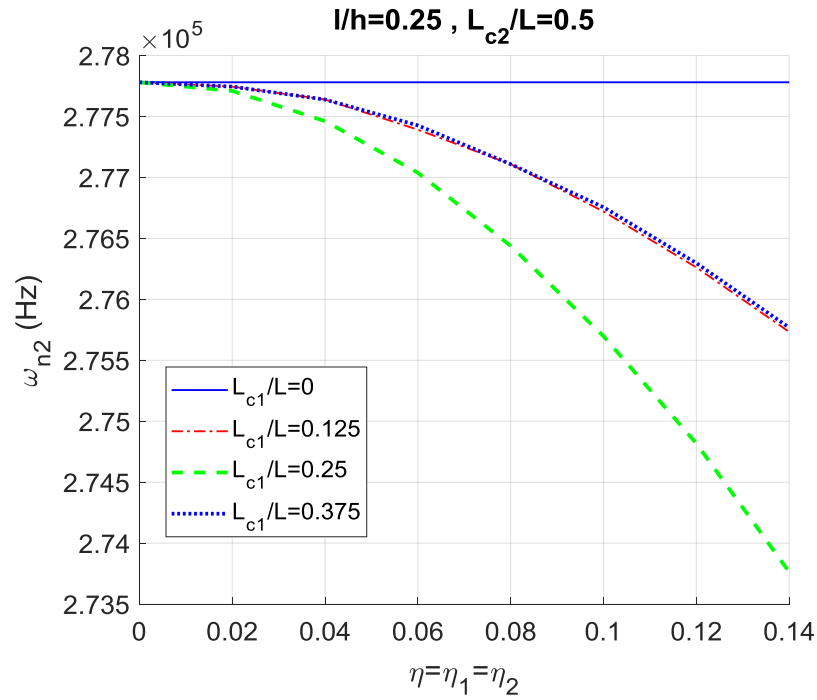
Fig. 7: Variation of the second natural frequency versus the crack depth ratio with the various first crack location
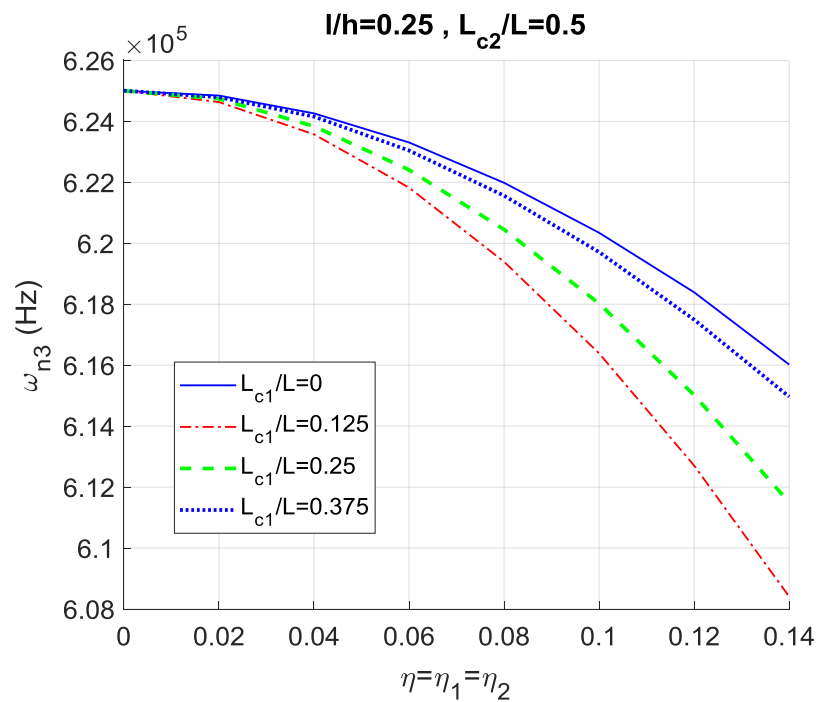

Fig. 8: Variation of the third natural frequency versus the crack depth ratio with the various first crack location
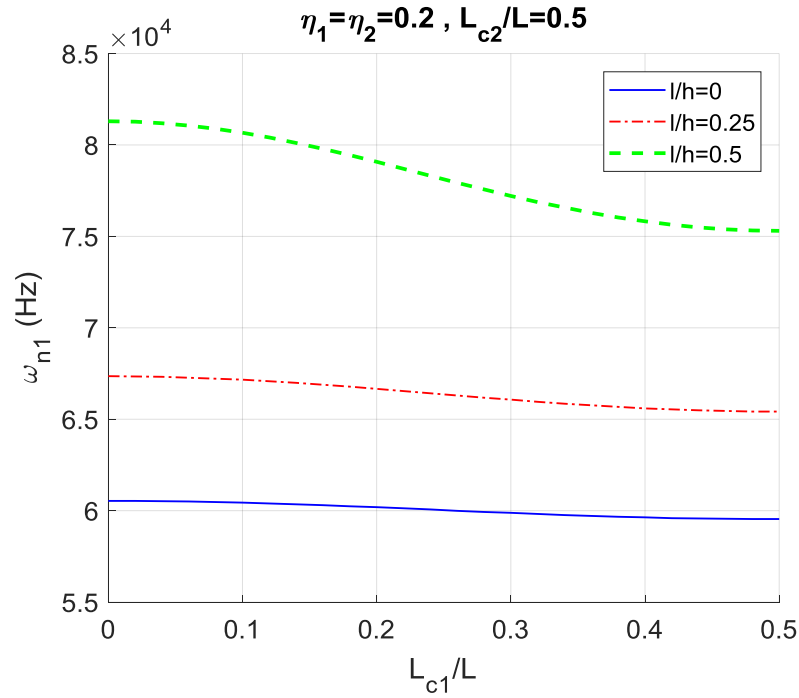
Fig. 9: Variation of the first natural frequency versus the first crack location with three different values of the material-length-scale parameter
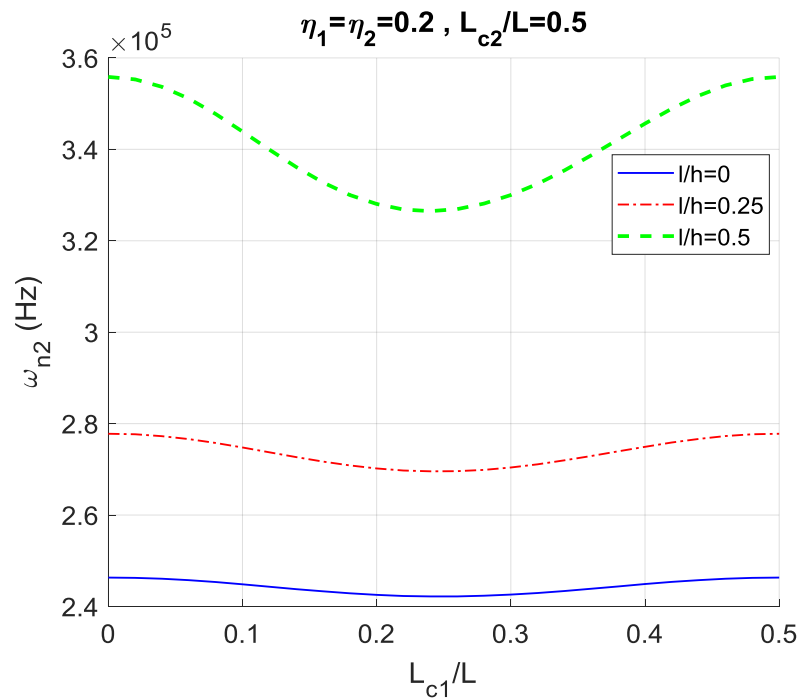

Fig. 10: Variation of the second natural frequency versus the first crack location with three different values of the material-length-scale parameter
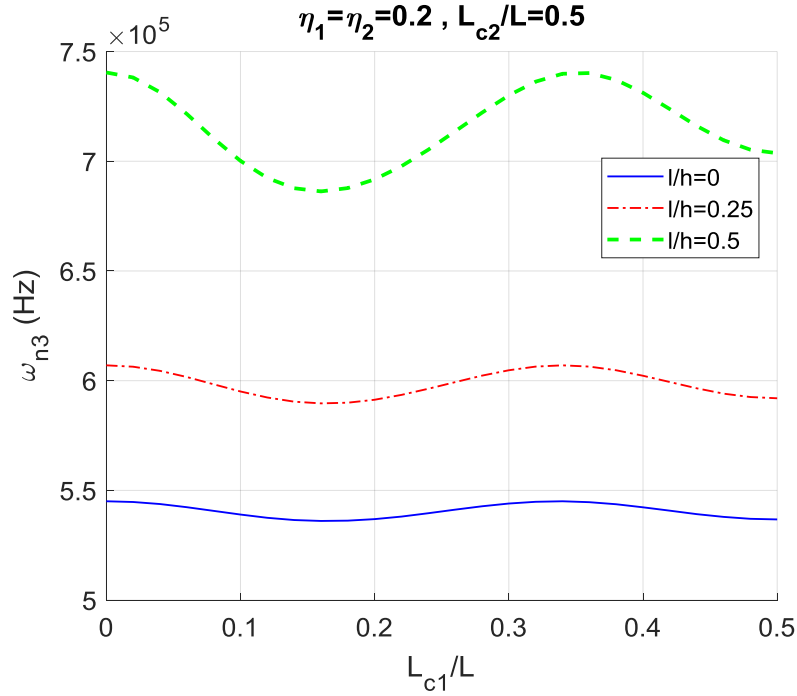
Fig. 11: Variation of the third natural frequency versus the first crack location with three different values of the material-length-scale parameter

7. Verification

In a special case, if $\frac{l}{h} \approx 0$, the microbeam is converted to a macro system and also by neglecting cracks in the beam by substituting $\eta = 0$, the system will be converted to a simple Euler-Bernoulli beam problem without any crack. Therefore, in Figs. 3, 4 and 5, the intersection of the blue line curves with the vertical axis must be exactly equal to natural frequencies of the simply-supported Euler-Bernoulli beam as follows[39]:

$$\omega_n(Hz) = \left(\frac{1}{2\pi}\right)(\beta_n L)^2 \left(\frac{EI}{\rho A L^4}\right)^{\frac{1}{2}}; \quad \beta_n L = n\pi \; ; \quad (n = 1, 2, \dots) \tag{18}$$

By replacing mechanical properties and dimensions of the beam, the first three natural frequencies of the system can be calculated as follows:

$$\omega_{n1} = \left(\frac{1}{2\pi}\right)(\pi)^2 \left(\frac{EI}{\rho A L^4}\right)^{\frac{1}{2}} = 6.1580 * 10^4 \; (Hz)$$

$$\omega_{n2} = \left(\frac{1}{2\pi}\right)(2\pi)^2 \left(\frac{EI}{\rho A L^4}\right)^{\frac{1}{2}} = 4\omega_{n1} = 2.4632 * 10^5 \; (Hz) \tag{19}$$

$$\omega_{n3} = \left(\frac{1}{2\pi}\right)(3\pi)^2 \left(\frac{EI}{\rho A L^4}\right)^{1/2} = 9\omega_{n1} = 5.5422 * 10^5 \; (Hz)$$

The above analytical results exactly are equal to the frequencies of the blue line curves in Figs. 3, 4 and 5, respectively.

Also for macro beam cases (or if $\frac{l}{h} \approx 0$), according to Eq. (7) then $S \approx EI$. In these cases, the general solution of Eqs. (11) and boundary conditions Eqs. (16) will be exactly equal to the general solution and boundary conditions of Yoon *et al*. [37] that investigated the free vibration of double cracks a simply-supported Euler-Bernoulli beam.

In addition, by assuming a single crack in the system, governing equations of boundary conditions of Eqs. (12), (13) are written as follows:

$$W_1(0) = 0 \;\; ; \;\; \frac{d^2 w_1}{dx^2}(0) = 0$$

$$W_2(L) = 0 \;\; ; \;\; \frac{d^2 w_2}{dx^2}(L) = 0 \tag{20}$$

$$W_1(L_{c1}) = W_2(L_{c1})$$

$$\frac{dw_2}{dx}(L_{c1})) - \frac{dw_1}{dx}(L_{c1}) = \frac{d^2 w_1}{dx^2}(L_{c1}) \times \frac{S}{K_{ti}}$$

$$S\frac{d^2 w_1}{dx^2}(L_{c1}) = S\frac{d^2 w_2}{dx^2}(L_{c1}) \tag{21}$$

$$S\frac{d^3 w_1}{dx^3}(L_{c1}) = S\frac{d^3 w_2}{dx^3}(L_{c1})$$

Eqs. (20), (21) exactly are equal to boundary conditions of Rahi [21] that researched on the effect

of a crack on a simply-supported micro beam where $L_c = L_{c1}$.

8. Conclusion

In this paper, a simply-supported microbeam with multiple cracks was studied. In addition, based on MCST, the lateral dynamic behavior of the microbeam with Euler-Bernoulli model was investigated. First, every open edge crack was considered with a torsional spring based on MCST. Then, the governing equations of motion and boundary conditions of the system were obtained using Hamilton's principle. The governing equations were solved by the separating variables method. After that, the natural frequencies of the system were analytically calculated. Finally, numerical results were presented for the microbeam with two open-edge cracks. The results show that the depth of the cracks, the location of cracks, and material length scale parameter are extremely effective on the natural frequencies of the system.

References

[1] R.A. Coutu Jr, P.E. Kladitis, L.A. Starman, J.R. Reid, A comparison of micro-switch analytic, finite element, and experimental results, Sensors and Actuators A: Physical, 115 (2004) 252-258.

[2] V.R. Mamilla, K.S. Chakradhar, Micro machining for micro electro mechanical systems (MEMS), Procedia materials science, 6 (2014) 1170-1177.

[3] S. Kong, S. Zhou, Z. Nie, K. Wang, The size-dependent natural frequency of Bernoulli–Euler micro-beams, International Journal of Engineering Science, 46 (2008) 427-437.

[4] S.K. Park, X.L. Gao, Bernoulli–Euler beam model based on a modified couple stress theory, Journal of Micromechanics and Microengineering, 16 (2006) 2355.

[5] M.H.F. Dado, O. Abuzeid, Coupled transverse and axial vibratory behaviour of cracked beam with end mass and rotary inertia, Journal of sound and vibration, 261 (2003) 675-696.

[6] K.S. Al-Basyouni, A. Tounsi, S.R. Mahmoud, Size dependent bending and vibration analysis of functionally graded micro beams based on modified couple stress theory and neutral surface position, Composite Structures, 125 (2015) 621-630.

[7] X. Li, L. Li, Y. Hu, Z. Ding, W. Deng, Bending, buckling and vibration of axially functionally graded beams based on nonlocal strain gradient theory, Composite Structures, 165 (2017) 250-265.

[8] N. Shafiei, M. Kazemi, L. Fatahi, Transverse vibration of rotary tapered microbeam based on modified couple stress theory and generalized differential quadrature element method, Mechanics of advanced materials and structures, 24 (2017) 240-252.

[9] Y.-L. Zhang, J.-M. Wang, Exact controllability of a micro beam with boundary bending moment, International Journal of Control, (2017) 1-9.

[10] J. Fang, J. Gu, H. Wang, Size-dependent three-dimensional free vibration of rotating functionally graded microbeams based on a modified couple stress theory, International Journal of Mechanical Sciences, 136 (2018) 188-199.

[11] A. Babaei, M.R.S. Noorani, A. Ghanbari, Temperature-dependent free vibration analysis of functionally graded micro-beams based on the modified couple stress theory, Microsystem technologies, 23 (2017) 4599-4610.

[12] E. Taati, N. Sina, Multi-objective optimization of functionally graded materials, thickness and aspect ratio in micro-beams embedded in an elastic medium, Struct Multidisc Optim, 58 (2018) 265-285.

[13] M. AkbarzadehKhorshidi, M. Shariati, Buckling and postbuckling of size-dependent cracked microbeams based on a modified couple stress theory, Journal of Applied Mechanics and Technical Physics, 58 (2017) 717-724.

[14] M. Akbarzadeh Khorshidi, M. Shariati, A multi-spring model for buckling analysis of cracked Timoshenko nanobeams based on modified couple stress theory, Journal of Theoretical and Applied Mechanics, 55 (2017) 1127-1139.

[15] A.S.Y. Alsabbagh, O.M. Abuzeid, M.H. Dado, Simplified stress correction factor to study the dynamic behavior of a cracked beam, Applied Mathematical Modelling, 33 (2009) 127-139.

[16] B. Panigrahi, G. Pohit, Effect of cracks on nonlinear flexural vibration of rotating Timoshenko functionally graded material beam having large amplitude motion, Proceedings of the Institution of Mechanical Engineers, Part C: Journal of Mechanical Engineering Science, 232 (2018) 930-940.

[17] M. Soltanpour, M. Ghadiri, A. Yazdi, M. Safi, Free transverse vibration analysis of size dependent Timoshenko FG cracked nanobeams resting on elastic medium, Microsystem Technologies, 23 (2017) 1813-1830.

[18] S.D. Akbas, Free vibration of edge cracked functionally graded microscale beams based on the modified couple stress theory, International Journal of Structural Stability and Dynamics, 17 (2017) 1750033.

[19] N.N. Huyen, N.T. Khiem, Frequency analysis of cracked functionally graded cantilever beam, Vietnam Journal of Science and Technology, 55 (2017) 229.

[20] R.K. Behera, A. Pandey, D.R. Parhi, Numerical and experimental verification of a method for prognosis of inclined edge crack in cantilever beam based on synthesis of mode shapes, Procedia Technology, 14 (2014) 67-74.

[21] A. Rahi, Crack mathematical modeling to study the vibration analysis of cracked micro beams based on the MCST, Microsystem Technologies, 24 (2018) 3201-3215.

[22] A. Mofid Nakhaei, M. Dardel, M.H. Ghasemi, Modeling and frequency analysis of beam with breathing crack, Archive of Applied Mechanics, 88 (2018) 1743-1758.

[23] C. Fu, Y. Wang, D. Tong, Stiffness Estimation of Cracked Beams Based on Nonlinear Stress Distributions Near the Crack, Mathematical Problems in Engineering, 2018 (2018).

[24] A. Khnaijar, R. Benamar, A new model for beam crack detection and localization using a discrete model, Engineering Structures, 150 (2017) 221-230.

[25] A. Greco, A. Pluchino, F. Cannizzaro, S. Caddemi, I. Caliò, Closed-form solution based Genetic Algorithm Software: Application to multiple cracks detection on beam structures by static tests, Applied Soft Computing, 64 (2018) 35-48.

[26] K.V. Nguyen, Q. Van Nguyen, Element stiffness index distribution method for multi-crack detection of a beam-like structure, Advances in Structural Engineering, 19 (2016) 1077-1091.

[27] U. Andreaus, P. Baragatti, P. Casini, D. Iacoviello, Experimental damage evaluation of open and fatigue cracks of multi-cracked beams by using wavelet transform of static response via image analysis, Structural Control and Health Monitoring, 24 (2017) e1902.

[28] S. Ghadimi, S.S. Kourehli, Multi cracks detection in Euler-Bernoulli beam subjected to a moving mass based on acceleration responses, Inverse Problems in Science and Engineering, 26 (2018) 1728-1748.

[29] K. Zhang, X. Yan, Multi-cracks identification method for cantilever beam structure with variable cross-sections based on measured natural frequency changes, Journal of Sound and Vibration, 387 (2017) 53-65.

[30] H. Chouiyakh, L. Azrar, K. Alnefaie, O. Akourri, Vibration and multi-crack identification of Timoshenko beams under moving mass using the differential quadrature method, International Journal of Mechanical sciences, 120 (2017) 1-11.

[31] N.T. Khiem, N.T.L. Khue, Change in mode shape nodes of multiple cracked bar: I. The theoretical study, Vietnam Journal of Mechanics, 35 (2013) 175-188.

[32] N.T. Khiem, L.K. Toan, N.T.L. Khue, Change in mode shape nodes of multiple cracked bar: II. The numerical analysis, Vietnam Journal of Mechanics, 35 (2013) 299-311.

[33] S. Caddemi, I. Caliò, F. Cannizzaro, A. Morassi, A procedure for the identification of multiple cracks on beams and frames by static measurements, Structural Control and Health Monitoring, 25 (2018) e2194.

[34] M. Shoaib, N.H. Hamid, M.T. Jan, N.B.Z. Ali, Effects of crack faults on the dynamics of piezoelectric cantilever-based MEMS sensor, IEEE Sensors Journal, 17 (2017) 6279-6294.

[35] N.T. Khiem, D.T. Hung, A closed-form solution for free vibration of multiple cracked Timoshenko beam and application, Vietnam Journal of Mechanics, 39 (2017) 315-328.

[36] F. Cannizzaro, A. Greco, S. Caddemi, I. Caliò, Closed form solutions of a multi-cracked circular arch under static loads, International Journal of Solids and Structures, 121 (2017) 191-200.

[37] H.I. Yoon, I.S. Son, S.J. Ahn, Free vibration analysis of Euler-Bernoulli beam with double cracks, Journal of mechanical science and technology, 21 (2007) 476-485.

[38] T.V. Lien, N.T. Đuc, N.T. Khiem, Mode Shape Analysis of Multiple Cracked Functionally Graded Timoshenko Beams, Latin American Journal of Solids and Structures, 14 (2017) 1327-1344.

[39] S.S. Rao, Vibration of continuous systems, Wiley Online Library, 2007.